Journal of Applied Polymer Science

Geometrical Dependence of Viscosity of Polymethylmethacrylate Melt in Capillary Flow

Xiang Lin,[1] Adrian Kelly,[2] Dongyun Ren,[1] Mike Woodhead,[2] Phil Coates,[2] Kuisheng Wang[1]

[1]College of Mechanical and Electrical Engineering, Beijing University of Chemical Technology, Chaoyang District, Beijing 100029, China

[2]IRC in Polymer Engineering, School of Engineering, Design & Technology, University of Bradford, Bradford BD7 1DP, West Yorkshire, United Kingdom

Correspondence to: Dongyun Ren (E-mail: dongyunr@163.com) or Kuisheng Wang (E-mail: wangks@mail.buct.edu.cn)

ABSTRACT: The shear viscosity of polymethylmethacrylate (PMMA) melt is particularly investigated by using a twin-bore capillary rheometer at four temperatures of 210, 225, 240, and 255°C with different capillary dies. Experimental results show that the geometrical dependence of shear viscosity is significantly dependent on melt pressure as well as melt temperature. The measured shear viscosity increases with the decrease of die diameter at lower temperatures (210 and 225°C) but decreases with the decrease of die diameter at higher temperatures (240 and 255°C). Based on the deviation of shear viscosity curves and Mooney method, negative slip velocity is obtained at low temperatures and positive slip velocity is obtained at high temperatures, respectively. Geometrical dependence and pressure sensitivity of shear viscosity as well as temperature effect are emphasized for this viscosity deviation. Moreover, shear viscosity curve at 210°C deviates from the power law model above a critical pressure and then becomes less thinning. Mechanisms of the negative slip velocity at low temperatures are explored through Doolittle viscosity model and Barus equation, in which the pressure drop is used to obtain the pressure coefficient by curve fitting. Dependence of pressure coefficient on melt temperature suggests that the pressure sensitivity of shear viscosity is significantly affected by temperature. Geometrical dependence of shear viscosity can be somewhat weakened by increasing melt temperature. © 2013 Wiley Periodicals, Inc. J. Appl. Polym. Sci. 130: 3384–3394, 2013

KEYWORDS: viscosity and viscoelasticity; rheology; extrusion; properties and characterization

Received 22 April 2013; accepted 27 May 2013; Published online 17 June 2013
DOI: 10.1002/app.39591

INTRODUCTION

Flows of polymer melts in micro-injection (MI) or hot melt micro-extrusion (HMME) are microscopic flows. Development of micro-electro-mechanical systems (MEMS) facilities the application and the study of the microscopic flow of polymeric melts, especially formation of the molding of parts of micron dimension. The applicability of MEMS for many micro-products, such as high-precision light guiding plate, micro-heat transfer, and micro-sampling cell, has been extensively adopted with polymers. However, various studies have indicated that the flow behavior of polymeric melt through a microscopic scale channel is different from the flow behavior on the macroscopic scale.[1–3] The fact that rheological properties in micro-channels are significantly affected by many factors which could be micro-scale-dependent has been widely documented.[4–9] The flow profile in micro-scale channels, for example, was found to be different from that on the macron scale for polyethylenes.[10]

One of the important rheological parameters is the viscosity which shows the flow ability of fluid. However, the experimental viscosity value in practical processing could be significantly affected by the wall slip behavior. Using the Laser Doppler velocimetry (LDV) and a transparent slit die, the shear viscosity of a linear high density polyethylene (HDPE) melt was found to be about 40% higher with slip correction than that without correction.[11] However, similar phenomenon of the viscosity of acrylonitrile butadiene styrene (ABS) melt on the micron scale was not observed based on injection molding process without slip correction.[6,12–14] It was found that the measured viscosity of ABS were significantly lower (about 30–80% lower) than those obtained from conventional capillary rheometers on the macroscopic scale over the tested shear rate range and the apparent shear viscosity of it decreased with the decrease of capillary dimensions.

Behavior of wall slip and geometrical dependence of shear viscosity of polymer melts on the flow channel present complex

variations. Komuro et al.[7] investigated the wall slip and flow instability of a short branching polystyrene (PS). Based on a modified Mooney method, the slip velocity appeared to increase with increasing melt temperature and the critical slip stress above which a slip occurred decreased. Such slip phenomenon of linear polymers with relatively narrow molecular weight distribution has been extensively reported in the literatures.[11,14–19] However, mechanisms of wall slip are quite different for different polymers. Dependence of shear and extensional viscosities of hydroxypropyl cellulose (HPC) on strain rate and melt temperature was experimentally studied by Paradkar et al.[8] Apart from the shear-thinning, the measured shear viscosity was found to deviate from the power law was observed above the shear rate of 10^5 s^{-1}.

The wall slip of HDPE melt was also studied by Hatzikiriakos et al.[20] using a capillary rheometer. Effects of die scale and melt pressure on slip velocity in micro-channels were investigated. For the linear HDPE, Münstedt and Robert et al.[11,21] pointed out that the decrease of shear viscosity on the microscopic scale largely resulted from the increase of slip velocity at wall. The velocity distributions observed in their experiment were close to plug flow after a critical shear stress owing to strong slip. Corrected with the slip effect, the shear viscosity of polyethylenes (PE) on the microscopic scale can be higher than that on the macroscopic scale.[22] Different from the polyolefins in capillary extrusion, however, the shear viscosity of PMMA increased with the decrease of the scale of capillary die. Zhao et al.[23] measured the geometrical dependence of shear viscosity of PMMA, which was thought to be conduced by the slip layer between the bulk flow and the wall and corrected the slip velocity based on the entanglement–disentanglement mechanism. However, the mechanism of geometrical dependence of shear viscosity should be explored deeply and comprehensively. For most polymers, shear-thickening can be easily observed at an ultra high strain rate after reaching the quasi-Newtonian plateau at the shear rate of 10^6-10^7 s^{-1}. [24] The PMMA melt showed a much stronger shear-thickening effect than that of HDPE, low density polyethylene (LDPE) and polypropylene (PP), etc. Shear thickening occurred to LDPE at shear rate up to 10^7 s^{-1} and to PMMA the critical shear rate was close to 10^6 s^{-1}.

As expressed above, the wall slip plays an important role in the capillary extrusion flow and would account for a significant percentage in the whole flow velocity. Rides et al.[25] found that in one case the slip velocity almost accounted for 80% of the total bulk flow. This slip behavior leads to complications in both the measurement and the modelling of flow behavior. Theoretically, linear polymers with relatively narrow molecular weight distribution exhibit oscillating melt fracture over a wider range of shear rate. Stick-slip behavior causes flow discontinuity and finally results in strong slip. This phenomenon was nominally treated as a shear thinning effect in some studies.[15] Dependence of shear viscosity on melt pressure during the die extrusion is also another key factor. This effect was investigated for many various polymers in the past, such as LDPE, HDPE, PMMA, ABS, polycarbonate (PC), and PP, etc.[26–29] Each polymer could present different critical pressure coefficient to shear viscosity, and then shows different geometrical dependence of shear viscosity. The pressure sensitivity is mainly due to the decrease of the action of distance between molecules. For the capillary flow of polymer melts in practical processing, the shear rate could be high up to 10^6 s^{-1} companied by a high pressure, especially in micro-extrusion and micro-injection.

Due to the different deviation behavior of shear viscosity during capillary flows, special attention was given to the capillary flow behavior of molten PMMA through a twin-bore capillary rheometer for investigating the geometrical dependence of shear viscosity in this article. The dependence of both wall slip behavior and shear viscosity on capillary diameter and melt temperature as well as melt pressure was studied. According to the power law model, the geometrical dependence of shear viscosity was first measured at different melt temperatures through five pairs of capillary dies. Then, the slip velocity of PMMA melt in these capillary dies was compared according to the Mooney method. Limitation of Mooney method in calculating the slip velocity was found at low melt temperatures and negative slip velocities were obtained. The results showed that this limitation was relevant to the melt pressure sensitivity of shear viscosity, especially at low melt temperature. Repeatedly measurements with only one charge of barrel were further conducted with the $D = 0.25$ mm die for understanding the pressure sensitivity of shear viscosity, and then the pressure coefficients were calculated based on Barus equation.

EXPERIMENTAL

Materials

A polymethylmethacrylate (PMMA, grade VH067A) with a weight average molecular weight of 92,000 g mol^{-1}, a molecular weight distribution of 1.937, and a density of about 1.188–1.225 g cm^{-3} was obtained from Mitsubishi Rayon Co., Japan. This PMMA is a linear polymer with short branching and was supplied in pellet form. The polymer pellets should be dried in an oven at 90°C for at least 5 h before rheological testing.

Twin-Bore Capillary Rheometer

A twin-bore RH10 capillary rheometer (BOHLIN INSTRUMENTS, UK) was adopted in this experiment. Capillary dies with diameters $D = 0.25$, 0.50, 1.00, 1.50, and 2.00 mm were used. All capillary dies have the same die entry angle of 180° and a uniform aspect ratio of 16. Compared with a single-bore capillary rheometer, the twin-bore capillary rheometer is fitted with an additional orifice die of effectively zero length (ratio of length to diameter L/D is smaller than 0.25). The RH10 twin-bore capillary rheometer is a piston-driven, constant speed capillary rheometer. The plunger speed allows apparent shear rates ranging from 20 s^{-1} to 2×10^6 s^{-1} with different scales of capillary diameter. Melt temperature can be controlled within ±0.3°C of the set values and monitored by platinum resistance thermometers fitted in the three (top, middle, and bottom) zones of the barrel. Before the test started, the polymer, for example the PMMA melt in this article, was subjected to two pre-compression stages to a pressure of 0.25 MPa at large scale diameters ($D \geq 1.00$ mm) for 10 min and 0.50 MPa at small scale diameters ($D < 1.00$ mm) for 10 min. The equilibrium mode was carried out by the pressure stability with a pressure deviation of 0.5% by eight average samples. The twin-bore

Applied Polymer SCIENCE

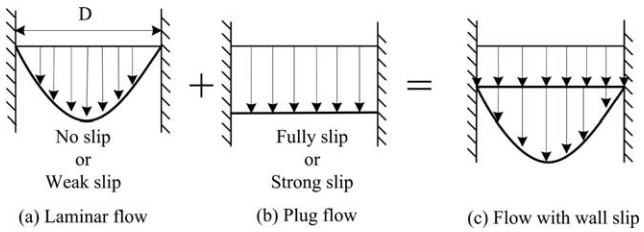

Figure 1. Schematic of slip behavior in circular channel: D is the diameter of channel.

rheometer is run in discrete speeds according to the apparent shear rates. The Cogswell method for calculating extensional viscosity is possible only in a twin-bore capillary rheometer, which allows two dies with different geometries to be examined simultaneously. The true pressure drop ΔP (Pa) through a capillary die is obtained by subtracting the measured pressure drop through the orifice die (P-right) from the measured pressure drop through the long capillary die (P-left). Thus, the corrected shear viscosity can be obtained in only one single test. The apparent shear rate $\dot{\gamma}_{app}$ (s^{-1}) and shear stress τ_w (Pa) can be expressed as eqs. (1) and (2), respectively.[30, 31]

$$\dot{\gamma}_{app} = \frac{4Q}{\pi R^3} \tag{1}$$

$$\tau_w = \frac{R\Delta P}{2L} \tag{2}$$

Rabinowitsch correction is used to obtain the shear rate $\dot{\gamma}_w$ (s^{-1}) at the wall for non-Newtonian liquids:

$$\dot{\gamma}_w = \frac{4Q}{\pi R^3}\left(\frac{3n+1}{4n}\right). \tag{3}$$

And then the shear viscosity η_s (Pa·s) can be calculated by

$$\eta_s = \frac{\tau_w}{\dot{\gamma}_w}. \tag{4}$$

In these equations, n is the non-Newtonian index, R is the radius (m) of the capillary having a length of L (m), and Q is the volumetric flow rate ($m^3\ s^{-1}$) through the capillary under a pressure drop ΔP (Pa) along the capillary. In addition, the principle of calculating extensional viscosity is based on the Cogswell's entrance effect by using the twin-bore capillary rheometer, which was given as:

$$\dot{\varepsilon} = \frac{4\eta_s \dot{\gamma}_w^{\,2}}{3(n+1)\Delta P_e} \tag{5}$$

and

$$\eta_e = \frac{9(n+1)^2(\Delta P_e)^2}{32\eta_s \dot{\gamma}^2}, \tag{6}$$

where $\dot{\varepsilon}$ is extensional rate (s^{-1}), ΔP_e is entrance pressure drop (Pa) which measured from the orifice die, and η_e is extensional viscosity (Pa·s).

RESULTS AND DISCUSSION

The phenomenon that shear viscosity of polymer melts changes with the die diameter during capillary flow is defined as geometrical dependence of shear viscosity in this study. For the viscosity measurement with capillary rheometer, the factors affecting shear viscosity of polymer melts mainly contain flow behavior and external conditions. The former could include entrance effect, surface tension and wall slip, etc., and the latter may include melt temperature, melt pressure, and shear effect, etc. Shear heating effect during capillary extrusion is assumed to be neglected in this study. Therefore, melt temperature and pressure were considered as the dominant factors to shear viscosity.

Geometrical Dependence of Shear Viscosity and Wall Slip

Generally wall slip includes two modes, i.e. weak slip and strong slip, as shown in Figure 1. The laminar flow is namely treated as a flow without slip, and the plug flow is treated as full slip. For a long time, the dominant idea about the mechanism for slip on wall surface was adhesive failure at the polymer/wall interface.[32] An expression of critical shear stress for the onset of wall slip as a function of the apparent contact angle between polymer and wall surface was developed as a mechanism of stick-slip transition for polymer melts based on Brochard–de Gennes slip model and molecular chain dynamics at the die wall was proposed by Allal et al.[33] Another slip mechanism is due to flow-induced chain detachment/desorption at the polymer/wall interface and to disentanglement of the polymer chains in the bulk from a monolayer of polymer chains adsorbed at the interface. Under flow, the polymer molecules in the bulk are stretched and these in turn apply forces to the molecules at the interface through the entanglements. When these forces exceed a critical value some of the chains will be detached from the interface and as a result a weak slip occurred. When the shear stress is increased further at the point where sudden disentanglement takes place, a strong slip (plug flow) is obtained.[34] Strong slip results in a nearly plug flow, which has already been confirmed by Robert et al.[21] Therefore, it is necessary to correct the determination of the shear rate in microscopic scale channel under considering slip behavior. Other researchers[35,36] also suggested that the strong slip was the sudden disentanglement of the polymer chains in the bulk from those in a monolayer of polymer chains adsorbed at the wall. The slip mechanism could be different for different polymers.

The Mooney method[37] for steady-state flow of Newtonian fluid based on the momentum equation under slip boundary conditions can be used. The fluid is supposed to be incompressible and isothermal. Thus:

$$Q_{Total} = Q_{Shear} + Q_{Slip}, \tag{7}$$

where Q_{Total}, Q_{Shear}, and Q_{Slip} are total, shear, and slip volume flow rate (m^3/s^{-1}), respectively. For flow in a capillary with a die radius R (m), Q_{Slip} can be can be calculated by

$$Q_{Slip} = v_s\ \pi\ R^2, \tag{8}$$

where v_s is the slip velocity (m/s^{-1}). For the power-law fluid, shear viscosity can be written according to power-law model as

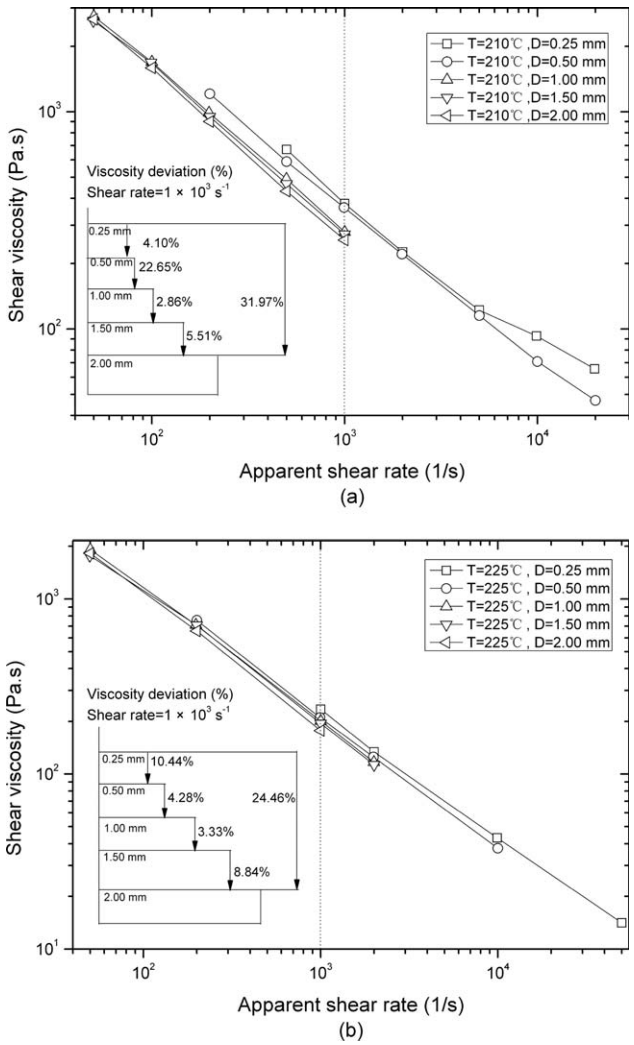

Figure 2. Shear viscosity of PMMA melts from different capillary dies: (a) $T = 210°C$; (b) $T = 225°C$.

$$\eta_s = K\dot{\gamma}_{\text{app}}{}^{n-1}, \tag{9}$$

where K is consistency index, $\dot{\gamma}_{\text{app}}$ is the apparent or Newtonian shear rate (s^{-1}) in eq. (1), and n is the non-Newtonian index. Based on Rabinowitsch correction,[38] relationship between the slip velocity and the apparent shear rate and true shear rate $\dot{\gamma}_{\text{true}}$ (s^{-1}) can be characterized by

$$\frac{4Q_{\text{total}}}{\pi R^3} = \frac{4v_s}{R} + \dot{\gamma}_{\text{true}}. \tag{10}$$

For a certain polymer flowing in a certain capillary, eq. (10) predicts that, for a given shear stress, a plot of apparent wall shear rate $4Q_{\text{Total}}/\pi R^3$ versus $1/R$ will has a gradient of $4v_s$ thus enabling the slip velocity to be determined.

The geometrical dependence of shear viscosity was firstly measured at 210 and 225°C. The five pairs of capillary dies were adopted for measuring the shear viscosity of PMMA under the same melt temperature. Shear rates were set at the same stages for comparing the deviation of shear viscosity. Figure 2 shows the difference among the curves of shear viscosity versus apparent shear rate. The Power Law viscosity model was used to fit the measured data and the PMMA melt exhibited typical pseudo-plastic shear-thinning behavior with shear rates up to 10^4 s^{-1}. Deviation percentages of viscosity value between the results tested by any two capillary dies (e.g., D_1 and D_2) at a constant shear rate of 1×10^3 s^{-1} are calculated, i.e., deviation percentage $= (1 - \eta_{D2}/\eta_{D1}) \times 100\%$. It can be found that the shear viscosity decreases with the increase of diameter of capillary die, especially at low melt temperatures. The deviation percentage of shear viscosity between dies of $D = 0.25$ mm and that of $D = 2.00$ mm is 31.97% at 210°C and that of 24.46% at 225°C. The geometrical dependence of shear viscosity is more significant at low temperature. Moreover, shear viscosity becomes less thinning above the shear rate of 5×10^3 s^{-1} at 210°C and the viscosity curves appear to deviate from the Power Law model, as shown in Figure 2(a). However, this deviation can not be observed from the curves measured at 225°C.

When the melt temperature increases to 240 and 255°C, the variation of shear viscosity versus apparent shear rate is contrary to those at 210 and 225°C, as shown in Figure 3. At 240

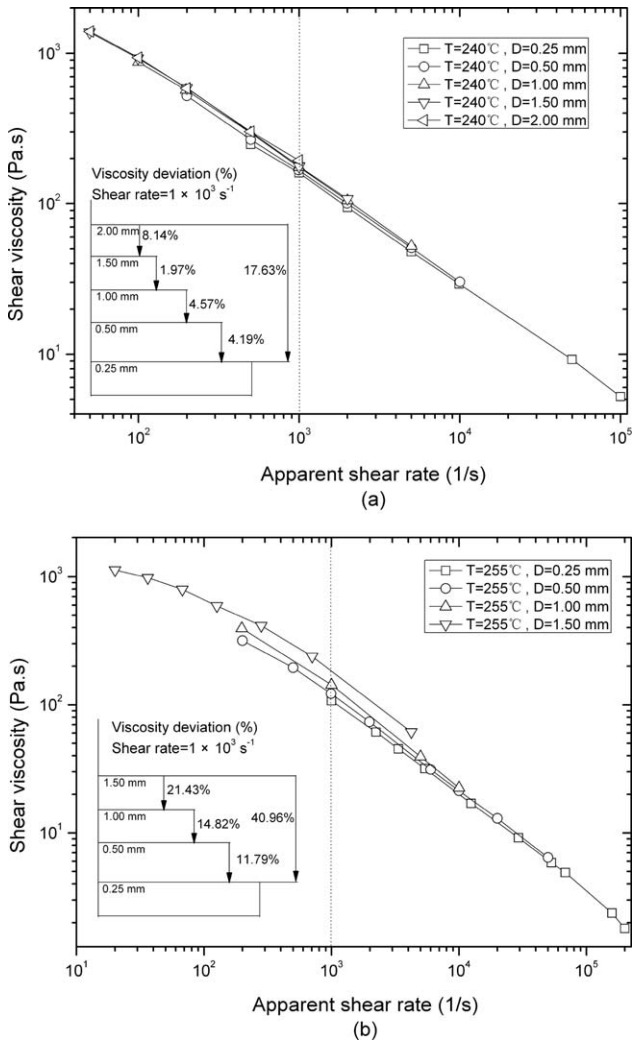

Figure 3. Shear viscosity of PMMA melts from different capillary dies: (a) $T = 240°C$; (b) $T = 255°C$.

Applied Polymer SCIENCE

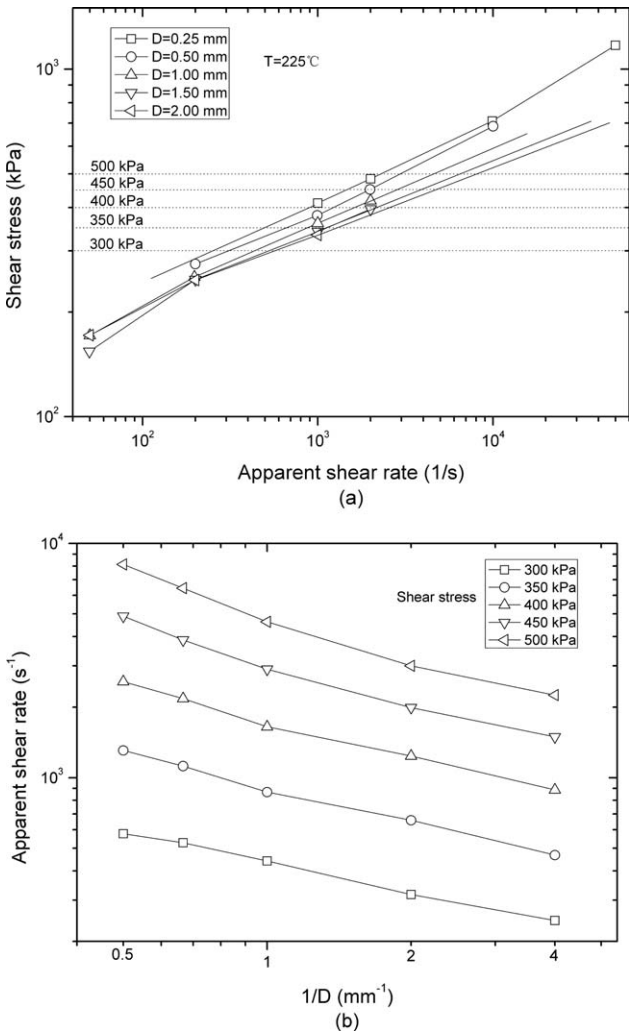

Figure 4. Plots based on the Mooney method at 225°C: (a) flow curves; (b) shear rate versus 1/*D*.

and 255°C, measured shear viscosity increases with the increase of diameter of capillary die. The tested viscosity values from different dies are close to each other at 240°C, but there still is a deviation percentage of 17.63% at 1×10^3 s^{-1} between the viscosities measured from $D = 0.25$ mm and that measured from $D = 2.0$ mm. For those measured at 255°C, the deviation percentage between the viscosity measured from $D = 0.25$ mm and that from $D = 1.50$ mm is up to 40.96%. Because the flow ability increases abruptly at 255°C and the melt pressure equilibrium is hard to balance, so the viscosity from the die of $D = 2.00$ mm at the melt temperature of 255°C is hardly measured within a similar range of shear rate. In addition, increasing temperature can effectively increasing the maximum shear rate in the die of 0.25 mm. The highest shear rate increases from 4×10^4 s^{-1} to 2×10^5 s^{-1} corresponding temperature from 210 to 255°C, respectively.

The most important point shown in Figure 3 is that the variation is totally different from that revealed in Figure 2. It seems that there should be a critical temperature between 225 and 240°C at which the deviation percentage of shear viscosity could be the minimum. The geometrical dependence is not significant anymore when the shear rate exceeds 1×10^4 s^{-1} at which the shear viscosity seems to be equal.

Some scholars suggested that the slip behavior appeared to be more significant in larger capillaries than in smaller capillaries and then the geometrical dependence of viscosity was attributed to the slip behavior at interface wall.[6,12–14] This could be effective to explain this phenomenon for polyethylenes and polypropylenes. When this deviation mechanism is used to explain the deviation for the PMMA, however, it is not working. The slip velocity should increase with the melt temperature and should account a larger part of the flow velocity. Then the variation trends at 240 and 255°C should be similar to those at 210 and 225°C, but the true situation is totally different from that. Based on the Mooney method, plots of shear stress versus apparent shear rate and plots of apparent shear rate versus 1/*D* at 225°C were carried out for determining the slip velocity, as shown in Figure 4. At a series of constant shear stress of 300, 350, 400, 450, and 500 kPa, the plots of apparent wall shear rate $4Q_{Total}/\pi R^3$ versus 1/*D* were conducted as shown in Figure 4(b). There are two points here which are against the regulation of Mooney method. First, the plots of apparent shear rate versus 1/*D* are not linear. Second, even though these plots can be fitted to be linear, the line slope which is relevant to the slip velocity v_s seems to be negative. As an absolute physical parameter, the value of v_s cannot be negative. If it is true, the PMMA melt will flow against the direction of impetus. Thus, the Mooney method does not fit to calculate the wall slip velocity for PMMA at this temperature of 225°C as well as 210°C.

Figure 5 shows the flow curves and the plots of apparent shear rate versus 1/*D* at three constant shear stresses at 240°C. It can be found that higher shear rate is obtained from the die of $D = 2.00$ mm at the same shear stress. Positive line slope can be obtained and then positive slip velocities by only taking account of the data from the capillary dies of $D = 0.50$, 1.00, and 1.50 mm. However, this is negative to explain the variation of the data from all of the dies. The difference revealed from Figure 4(b) and Figure 5(b) shows that there must be other significant factors which play a much more important role on the geometrical dependence of shear viscosity than the slip does. At a higher melt temperature, however, positive slip velocity can be calculated through the Mooney slip principle. Linear plots of shear stress versus apparent shear rate and of apparent shear rate versus 1/*D* at constant shear stresses at 255°C can be fitted in Figure 6. For the different slip velocity results on the temperatures, the pressure sensitivity of shear viscosity is proposed to be responsible for this difference.

Geometrical Dependence of Shear Viscosity and Melt Pressure

As characterized in the "Geometrical Dependence of Shear Viscosity and Wall Slip" section, the deviation behaviors of shear viscosity at the melt temperatures of 210 and 225°C are different from those at 240 and 255°C, so the pressure sensitivity of shear viscosity was particularly studied at 210 and 240°C as examples. In order to better understand why there is a different geometrical dependence of shear viscosity for PMMA, the shear

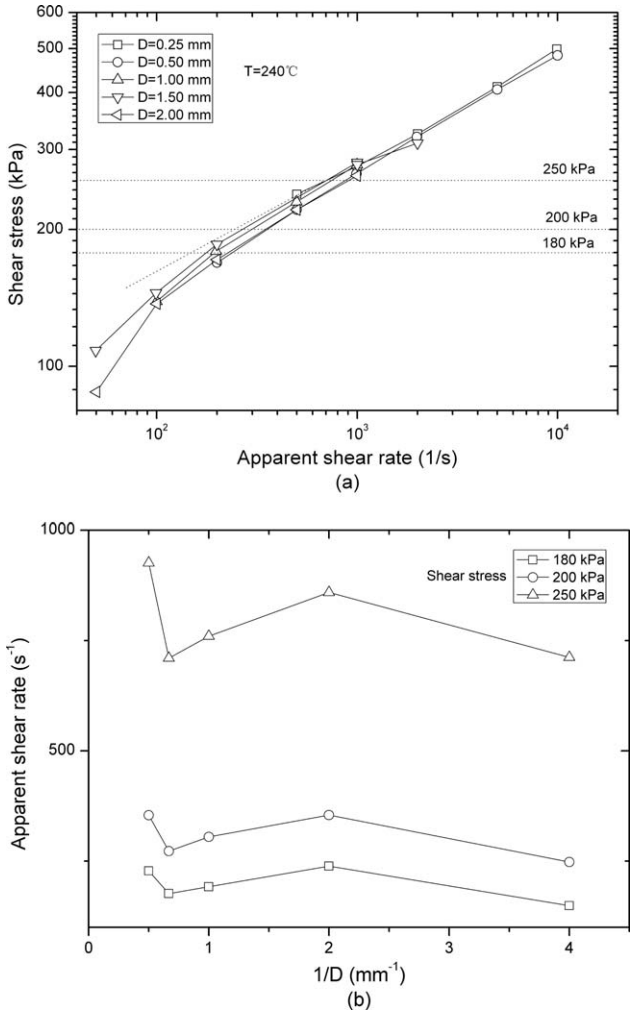

Figure 5. Plots based on the Mooney method at 240°C: (a) flow curves; (b) shear rate versus 1/*D*.

viscosity was repeatedly measured through the die of $D = 0.25$ mm by only using one barrel charge at 210 and 240°C, respectively. After finishing one capillary testing, the melt inner pressure was released fully and then another running was restarted immediately. Thus, the free volume among the PMMA molecular chains is compressed again and again, and then the density of it increases gradually. Figure 7 shows the pressure sensitivity results which were measured with the $D = 0.25$ mm capillary die under different pressures. Big difference of those plots measured at 210°C was shown in which the viscosity increases with the increase of the melt pressure. The pressure sensitivity is more significant at 210°C [Figure 7(a)] than that at 240°C [Figure 7(b)]. Under a high melt pressure up to approximately 180 MPa, the shear viscosity can be significantly increased from 26.9 to 65.5 Pa·s. That is because at a low melt temperature the melt pressure can be built up easily in the capillary flow. However, the flow ability of PMMA melt increases and it can be easier to flow through the capillary die at 240°C, and this causes the melt pressure hardly increases as that presents at 210°C. Thus, the viscosity curves are close to each other shown in Figure 7(b).

Figure 8 shows the plots of melt pressure from the long die versus shear viscosity. It can be found that plots of pressure P-long die versus shear viscosity are close to each other at low shear rate (high viscosity), even at 210°C. That means the pressure sensitivity plays a less significant role at low shear rate. The molecular chains are compressed closely and free-volume among them reduces to a relative minimum degree under super high pressure. Without high pressure, large difference between the curves can not be found at low shear rate. Even melt morphology could be found under low pressure and thus do not present large difference on the viscosity behavior. However, this situation at high shear rates can still be observed at 240°C [Figure 8(b)]. For example, the melt pressure tested at 210°C under a shear rate of 10^4 s^{-1} ranges from 78.2 to 126 MPa, then the viscosity ranges from 34.3 to 93.4 Pa·s. The 61.13% increase of melt pressure leads to a 172.30% increase of shear viscosity. When it comes to the melt temperature of 240°C, however, there is only 8.86% increase of shear viscosity corresponding to 17.47% increase of pressure at the same shear rate. The temperature effect on the pressure sensitivity is significant.

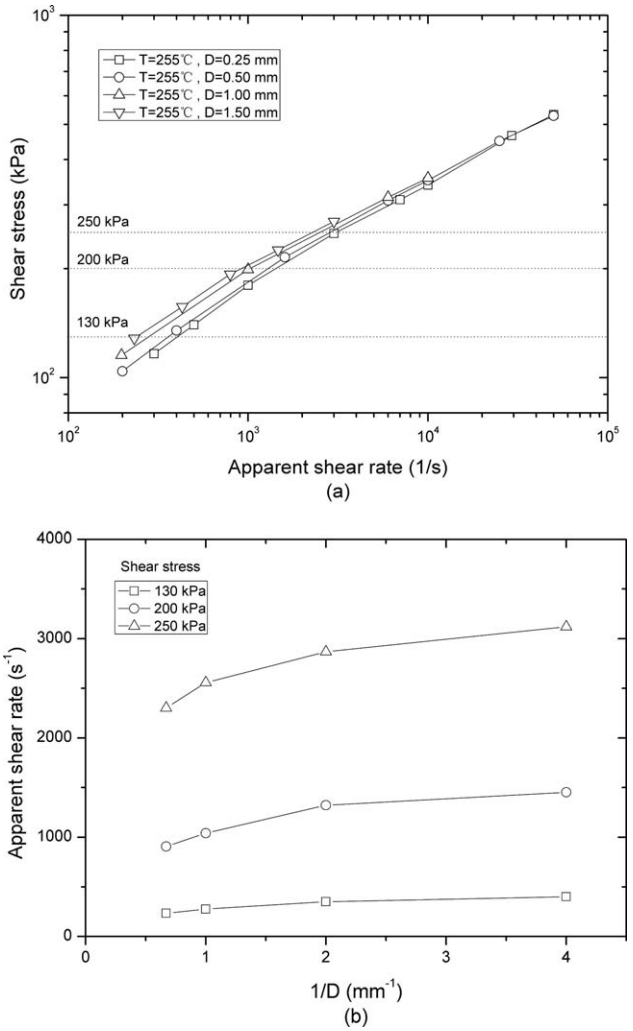

Figure 6. Plots based on the Mooney method at 255°C: (a) flow curves; (b) shear rate versus 1/*D*.

Applied Polymer SCIENCE

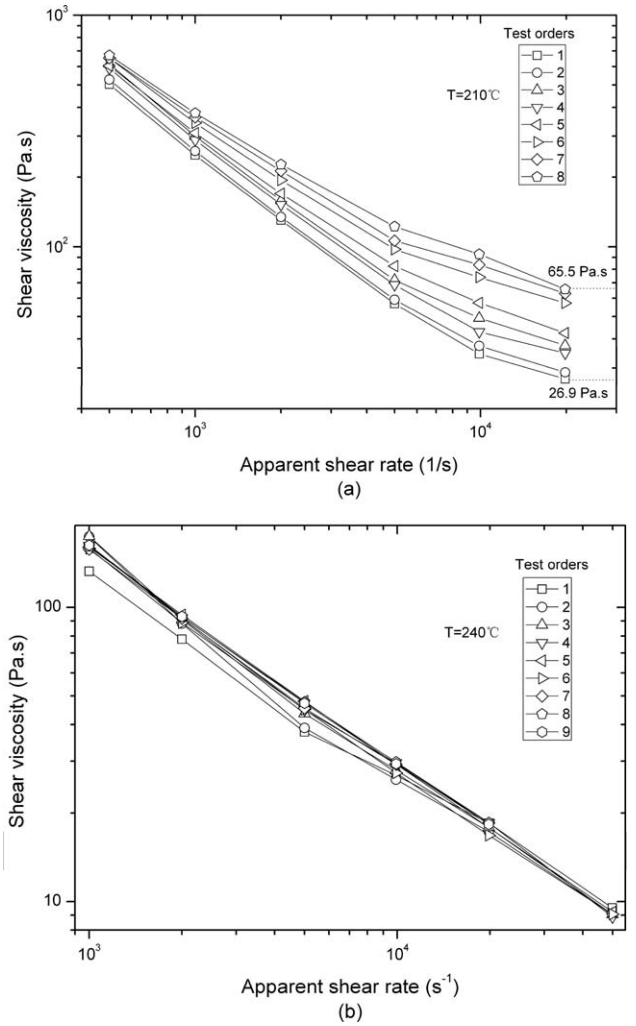

Figure 7. Shear viscosity measured through the die of $D = 0.25$ mm at (a) 210°C and (b) 240°C.

Results shown in Figures 7 and 8 clearly suggest that the pressure sensitivity plays a much more dominant role to the geometrical dependence of shear viscosity at 210°C than that at 240°C. Increasing melt temperature can effectively reduce the geometrical dependence of shear viscosity due to the decrease of melt pressure. Therefore, the true reason of the occurrence of negative slip at 210°C velocity is that the pressure sensitivity of PMMA covers the effect of slip behavior on the shear viscosity. If the effect of pressure sensitivity on shear viscosity can be overcome, the slip velocity can still be calculated.

Furthermore, relationship between the melt pressure in the long die and the shear viscosity tested from different capillary dies are further shown in Figure 9. It is shown that the melt pressure increases with the decrease of the die diameter at a constant shear viscosity at 210°C. The highest melt pressure at the same shear rate comes from the die of $D = 0.25$ mm. However, totally different situation happens at 240°C, as shown in Figure 9(b). The pressures from different dies are very close to each other. Significant increase of pressure can not be found and this leads to less obvious pressure sensitivity [Figure 3(a)]. In addition, for the pressure tested from the die of $D = 0.25$ mm, melt pressure deviates from the plotted line and goes fast up at 210°C below the shear viscosity of 100 Pa·s, which also can not be observed at 240°C.

GPC measurements were carried out for checking degradation during the capillary testing. Extrudates corresponding to the testing orders of 1, 2, 3, 6, 7, and 8 in Figure 7(a) were adopted as samples for these GPC measurements. Results shown in Table I suggest that minor degradation happens compared to the raw sample; however, large difference cannot be found among the samples from capillary extrusion. This reveals that the degradation during the capillary testing can be neglected and the deviation of shear viscosity shown in Figure 7(a) cannot be attributed to the molecular degradation.

The pressure sensitivity was also found to be linked to the molecular chains of polymers in the previous work.[24] Those polymers with large side chain groups (branching structure) had a higher sensitivity to melt pressure. The pressure effect, dependent on the molecular structure, plays an important role in the Newtonian plateau and shear-thickening. This is useful to

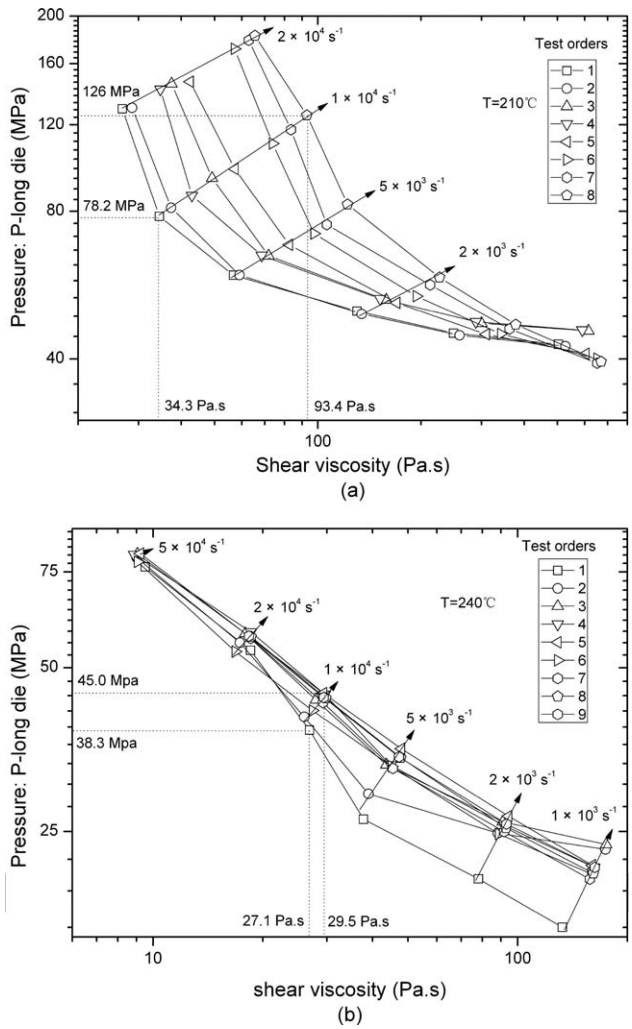

Figure 8. Plots of shear viscosity versus pressure-long die from the die of D=0.25 mm at (a) 210°C and (b) 240°C.

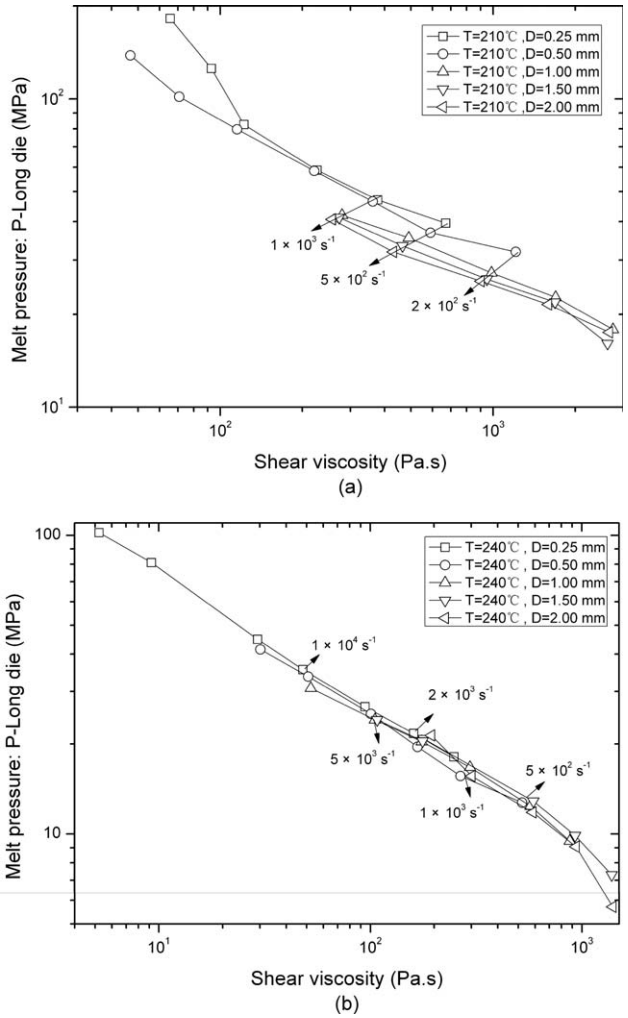

Figure 9. Plots of shear viscosity versus pressure-long die at (a) 210°C and (b) 240°C measured from different capillary dies.

explain why pressure sensitivity can be easily observed for PMMA and PS, but it hardly to be measured for the PE and PP which have higher linear level of molecular structures. Most of the viscosity equations and database in simulation software are based on an important assumption that the flowing fluid is incompressible. However, errors could be significant caused by the pressure sensitivity of viscosity. When the PMMA is used in MI processes at a low temperature, high pressure always happens and leads to increase flow resistance. Thus, pressure dependence of shear viscosity is important in process-design and simulation.

Table I. Details of M_w and M_w/M_n of samples at 210°C corresponding to Figure 7(a)

Testing orders	M_w (g mol^{-1})	M_w/M_n
1	90,793	2.074
2	90,339	2.193
3	90,002	2.108
6	89,784	2.130
7	88,952	2.148
8	89,841	2.090
Raw sample	92,000	1.937

The mechanism of pressure sensitivity of shear viscosity could be attributed to the increase/decrease of free-volume among the molecular chains. High melt temperature can effectively enhance the Brownian movement of molecular chains and then increase the free-volume, thus viscosity decreases. However, the pressure effect covers the temperature effect on shear viscosity under super high melt pressure. Thus the pressure sensitivity on shear viscosity is proposed to explain this phenomenon for PMMA in this work. Figure 10 shows the relationship between specific volume and melt temperature from the Moldflow database. As is described in Figure 10, increasing pressure decreases of specific volume, which results in high viscosity and flow resistance. According to the practical situation, comparison of dependence of melt pressure on specific volume under two melt pressures between 50 and 200 MPa is taken as examples. Significant dependence of specific volume on melt pressure is observed. Under high pressure, however, the fraction of free volume (FFV) should decrease, especially for those branching polymers.

For a better understanding of the above mentioned, the pressure sensitivity can also be explained by the Doolittle viscosity equation using a free volume component. Although the Doolittle viscosity model is an extension of the Arrhenius equation, modified to take into account the change of temperature with the free volume and the effect on the shear viscosity, it still could be used to characterize the effect of the free-volume on shear viscosity. It has the form[39]

$$\ln \eta = B\left(\frac{V_0}{V_f}\right) + \ln A \tag{11}$$

where η is the shear viscosity η_s (Pa·s) in this paper, A and B are constants, V_0 and V_f are the occupied volume (Å^3) of the molecular chains and free volume (Å^3), respectively. It can be

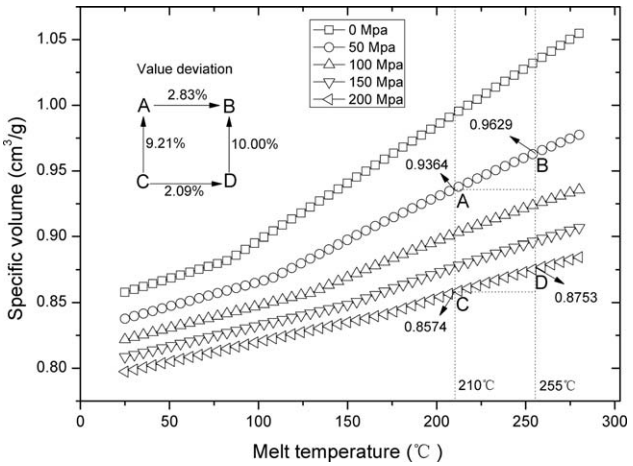

Figure 10. Plots of melt temperature versus specific volume under different pressures from Moldflow database: A, C are the points tested at 210°C under the melt pressure of 50 and 200 MPa, respectively and B, D are the points tested at 240°C under the melt pressure of 50 and 200 MPa, respectively.

Applied Polymer SCIENCE

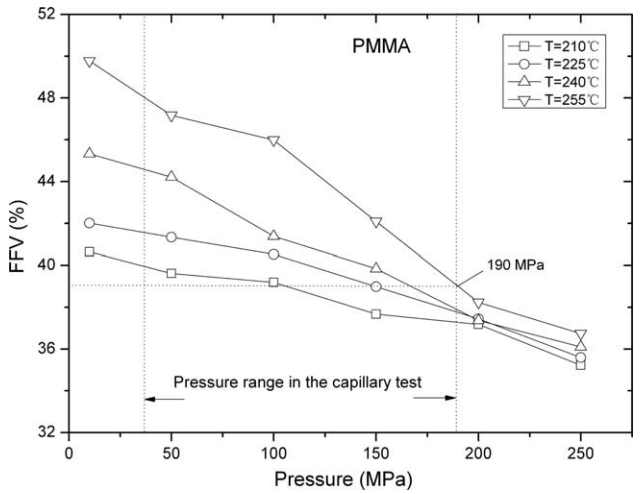

Figure 11. Molecular dynamics simulation of the FFV dependence on pressure and temperature from Material Studio®.

sure from eq. (11) that the V_f will decrease with increasing melt pressure and the ratio of V_0/V_f will increase definitely. Other models for explaining the pressure effect on the shear viscosity of polymers were proposed.[26,40] For instance, Liang[40] proposed the pressure coefficient β to describe the significance of pressure effect through die flows in which the melt pressure was less than 22 MPa (rubber). The value of β is dependent on the geometrical dimensions of dies and pressure distribution during capillary flow. Similar work was also conducted by Binding et al.[26] when they investigated the pressure dependence of viscosity under the pressures no more than 70 MPa, including shear viscosity and extensional viscosity, for five polymer melts. In this study, however, the melt pressure is up to 180 MPa, under which the FFV changes significantly, as shown in Figure 11. The FFV of the PMMA melt was considered through the molecular dynamics simulation based on the N–P–T assembling system. It is shown that temperature plays a significant role in the FFV and at high temperature, FFV decreases faster than that does at low temperature. Higher compressibility at higher temperature decreases the pressure which is required to push forward the flow of melt, thus the capillary behavior becomes less pressure sensitivity at high temperature.

Effect of Melt Temperature on the Pressure Sensitivity

Geometrical dependence of extensional viscosity of PMMA at different temperatures was also considered as an index of elasticity, as shown in Figure 12. Capillary dies of 0.25, 0.50, and 1.00 mm are used for this comparison. The resistance to extensional deformation of PMMA, which described by extensional viscosity, not only decreases with increasing of melt temperature but also generally decreases with increasing die diameter. This is helpful to reduce the pressure drop of entrance-flow, thus finally reduces the total pressure applied on the melt. Therefore, low melt pressure difference was observed under high temperature [Figures 8(b) and 9(b)].

The Barus equation can be used to describe the significance of pressure effect on the shear viscosity.[26] Here, the Barus equation modified for this work can be described as

$$\eta = \eta_{P_0} e^{\beta(\Delta P - P_0)}, \tag{12}$$

where η can be replaced by the shear viscosity η_s (Pa·s) in this article, η_{P0} is the shear viscosity (Pa·s) at atmospheric conditions, β is the pressure coefficient (GPa^{-1}), ΔP is melt pressure drop (GPa), and P_0 is the pressure around the flow outlet. In this study, the pressure P_0 is treated to be zero and the viscosity η_{P0} is constant for a given shear rate under given temperature. Then eq. (12) can be changed to

$$\ln \eta_s = \beta \Delta P + \ln \eta_{P_0}. \tag{13}$$

Therefore, eq. (13) predicts that, for a given shear rate, pressure coefficient β is relevant to the slope rate of the plot of logarithm shear viscosity ln η_s versus ΔP, thus enabling β to be determined. Thus, the pressure effect of shear viscosity can be directly estimated through this expression, as shown in Figure 13. The pressure coefficient β decreases significantly with increasing shear rate at both temperatures with different increasing magnitudes. Similar conclusion was also obtained in Liang's work.[40] Moreover, the value of β also decreases effectively with increasing temperature, especially at low shear rate. As aforementioned in Figure 7, more significant pressure sensitivity was observed at low temperature of 210°C. The ease of the temperature effect on the pressure sensitivity is positively shown in Figure 13. Under the same pressure, there is a lower density of melt at high temperature due to the higher FFV, as shown in Figure 11. Thus the flow melt is compressed much more and presents low pressure sensitivity at high temperature. In addition, pressure over the measured range at 210°C is much higher than that at 240°C during the 0.25 mm capillary flow. The former is ranging from 34.2 to 118.3 MPa [Figure 13(a)] and the latter is ranging from 12.9 to 38.9 MPa [Figure 13(b)], respectively. This finally leads to the different viscosity behaviors shown in Figure 7.

CONCLUSIONS

Using a standard capillary rheometer, dependence of shear viscosity on slip behavior, pressure sensitivity, and melt

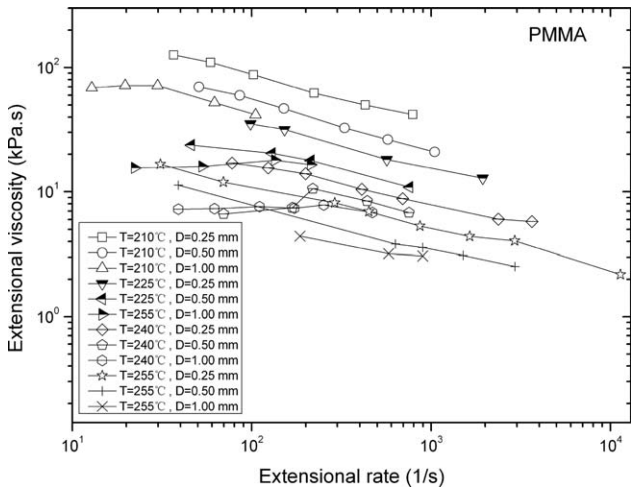

Figure 12. Extensional viscosities of PMMA under different temperatures.

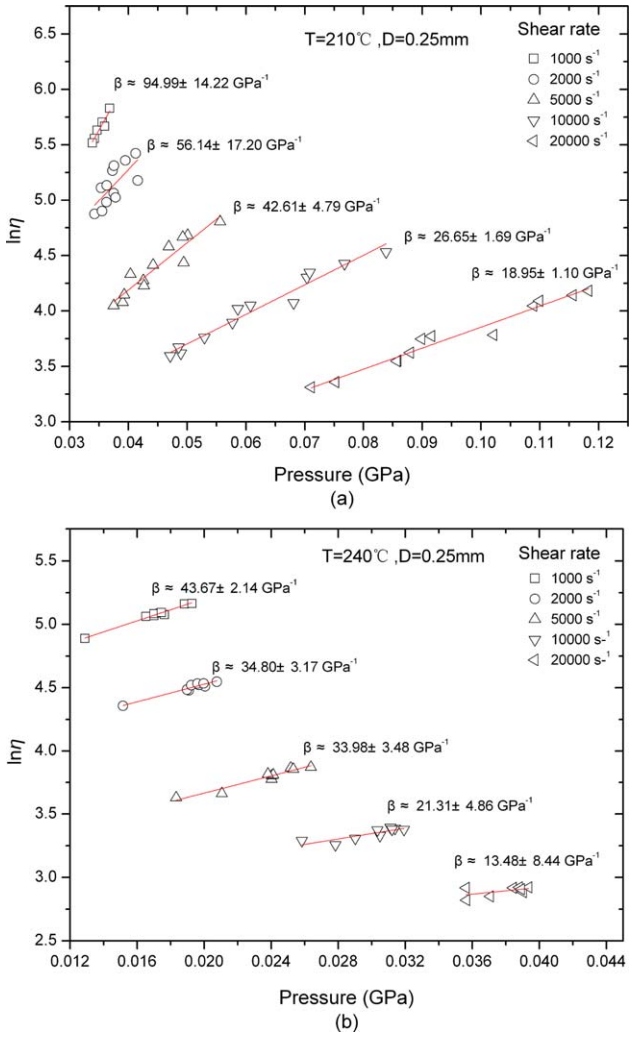

Figure 13. Analysis of pressure coefficient β at (a) 210°C and (b) 240°C. [Color figure can be viewed in the online issue, which is available at wileyonlinelibrary.com.]

temperature was studied in this study. The geometrical dependence of shear viscosity was investigated at four temperatures of 210, 225, 240, and 255°C. The tested shear viscosity decreases with increasing capillary diameter at low temperatures of 210 and 225°C whereas the shear viscosity increases with increasing capillary diameter at 240 and 255°C. Based on the Mooney method, negative slip velocity was found at 210°C and irregular plots of apparent shear rate versus $1/D$ were presented, but positive slip velocity was shown when the melt temperature increased to 255°C. The effect of melt pressure on shear viscosity is responsible to this phenomenon. The results of the intercomparison of dependence of shear viscosity of PMMA melt on the size of capillary die clearly demonstrate that wall slip could influence the shear viscosity results, but it is not dominant. Then the pressure sensitivity of shear viscosity was emphasized and the mechanism of geometrical dependence of shear viscosity was explored. Further investigation of the pressure sensitivity was conducted by repeatedly running the capillary testing through the die of $D = 0.25$ mm by only using one barrel charge at 210 and 240°C, respectively. Comparison of the plots of melt pressure versus shear viscosity tested by different capillary dies also showed that the pressure sensitivity could cover the effect of slip behavior on shear viscosity, especially at low melt temperatures. Finally, the melt temperature was found to show a significant influence on the extensional viscosity and pressure coefficient. Based on the Barus equation, pressure coefficient was calculated and the result showed that rising temperature can effectively decrease the pressure sensitivity of shear viscosity.

REFERENCES

1. Tsai, M. H.; Ou, K. L.; Huang, C. F.; Cheng, H. C.; Shen, K.; Chang, C. Y.; Wu, C. H.; Chen, J. H.; Guan, P. *J. Intern. Commun. Heat Mass. Transfer.* **2008**, *35*, 1097.
2. Song, M. C.; Liu, Z.; Wang, M. J.; Yu, T. M.; Zhao, D. Y. *J. Mater. Process Technol.* **2007**, 668, 187–188.
3. Sha, B.; Dimov, S.; Griffiths, C.; Packianather, M. S. *J. Mater. Process Technol.* **2007**, *183*, 284.
4. Ou, J.; Perot, B.; Rothstein, J. P. *Phys. Fluids* **2004**, *16*, 4635.
5. Gad el Hak; Macaque, M. *Industry* **2001**, *2*, 313.
6. Chen, S. C.; Tsai, R. I.; Chien, R. D.; Lin, T. K. *Intern. Commun. Heat Mass Transfer* **2005**, *32*, 501.
7. Komuro, R.; Kobayashi, K.; Taniguchi, T.; Sugimoto, M.; Koyama, K. *Polymer* **2010**, *51*, 2221.
8. Paradkar, A.; Kelly, A.; Coates, P.; York, P. *J. Pharm. Biomed. Anal.* **2009**, *49*, 304.
9. Harris, C.; Despa, M. S.; Kelly, K. W. *J. Microelectromech. Syst.* **2000**, *9*, 502.
10. Hatzikiriakos, S. G. *Prog. Polym. Sci.* **2012**, *37*, 624.
11. Münsted, A. H.; Schmidt, M.; Wassner, E. J. *J. Rheol.* **2000**, *44*, 413.
12. Chen, S. C.; Liao, W. H.; Yeh, J. P.; Chien, R. D. *Polym. Test.* **2012**, *31*, 864.
13. Chien, R. D.; Jong, W. R.; Chen, S. C. *J. Micromech. Microeng.* **2005**, *15*, 1389.
14. Chen, C. S.; Chen, S. C.; Liaw, L. W.; Chien, R. D. *Eur. Polym. J.* **2008**, 43, 1891.
15. Rosenbaum, E. E.; Hatzikiriakos, S. G.; Stewart, C. W. *Intern. Polym. Proc.* **1995**, *10*, 204.
16. Zhu, Z. Y. *Rheol. Acta* **2004**, *43*, 373.
17. Barone, J. R.; Wang, S. Q. *J. Non-Newt. Fluid. Mech.* **2000**, *91*, 31.
18. Delgadillo, V. O.; Hatzikiriakos, S. G. *Polym. Eng. Sci.* **2007**, *47*, 1317.
19. Delgadillo, V. O.; Hatzikiriakos, S. G. *Intern. Polym. Proc.* **2008**, *23*, 385.
20. Hatzikiriakos, S. G.; Dealy, J. M. *J. Rheol.* **1992**, *36*, 703.
21. Robert, L.; Demay, Y.; Vergnes, B. *Rheol. Acta* **2004**, *43*, 89.
22. Hatzikiriakos, S. G.; Kazatchkov, I. B.; Vlassopoulos, D. *J. Rheol.* **1997**, *41*, 1299.
23. Zhao, D.; Jin, Y.; Wang, M.; Song, M. *J. Mech. Eng. Sci.* **2010**, *225*, 1175.

24. Kelly, A. L.; Gough, T.; Whiteside, B. R.; Coates, P. D. *J. Appl. Polym. Sci.* **2009**, *114*, 864.
25. Rides, M.; Allen, C.; Fleming, D.; Haworth, B.; Kelly, A. *Polym. Test.* **2008**, *27*, 308.
26. Binding, D. M.; Couch, M. A.; Walters, K. *J. Non-Newt. Fluid Mech.* **1998**, *79*, 137.
27. Sedlacek, T.; Zatloukal, M.; Filip, P.; Boldizer, A.; Saha, P. *Polym. Eng. Sci.* **2004**, *44*, 1328.
28. Cardinaels, R.; Puyvelde, P. V.; Moldenaers, P. *Rheol. Acta* **2007**, *46*, 495.
29. Aho, J.; Syrjälä, S. *J. Appl. Polym. Sci.* **2010**, *117*, 1076.
30. Alexander, Y. M.; Avraam II. Rheology. Concepts, Methods, and Applications; ChemTech Publishing: Toronto, **2012**; Chapter 5, pp 257–269.
31. Gebhard S. A Practical Approach to Rheology and Rheometry; Gebrueder HAAKE GmbH: Germany, **2000**; Chapter 3, pp 70–81.
32. Hill, D. A.; Hasegawa, T.; Denn, M. M. *J. Rheol.* **1990**, *34*, 891.
33. Allal, A.; Vergnes, B. *J. Non-Newt. Fluid Mech.* **2012**, *46*, 167–168
34. Brochard, W. F.; de Gennes, P. G. *Langmuir* **1992**, *8*, 3033.
35. Drda, P. A.; Wang, S. Q. *Phys. Rev. Lett.* **1995**, *75*, 2698.
36. Allal, A.; Vergnes, B. *J. Non-Newt. Fluid Mech.* **2007**, *146*, 45.
37. Mooney, M. *J. Rheol.* **1931**, *2*, 210.
38. Rabinowitsch, B. Z. *Phys. Chem.* **1929**, *145*, 1.
39. Doolittle, A. K. *J. Appl. Phys.* **1951**, *22*, 1471.
40. Liang, J. Z. *Polymer* **2001**, *42*, 3709.